Permafrost Mapping through Multi-Source Geospatial Modeling

Sivatmiga T N
Department of Robotics and Automation Engineering
PSG College of Technology
Coimbatore, India
sivatmiga@gmail.com

Mullainathan V H
Department of Robotics and Automation Engineering
PSG College of Technology
Coimbatore, India
mullai2004@gmail.com

line 1: 3rd Given Name Surname
line 2: *dept. name of organization (of Affiliation)*
line 3: *name of organization (of Affiliation)*
line 4: City, Country
line 5: email address or ORCID

***Abstract*—Permafrost affects terrain stability and is a key factor in planning mobility in high-altitude regions. This study presents a modeling approach to estimate permafrost probability in the Western Himalayas (India) and Russian Arctic using satellite-based inputs and empirical thermal models. The workflow integrates digital elevation data, MODIS land surface temperature, NDVI, NDSI, ERA5 reanalysis temperature, and soil parameters from SoilGrids. After spatial preprocessing and alignment, three models are computed namely Temperature at the Top of Permafrost (TTOP), Mean Annual Ground Temperature (MAGT), and Active Layer Thickness (ALT). These outputs are normalized and combined to produce a continuous permafrost probability map, later classified into three zones such as high, moderate, and low confidence. Data processing and index derivation are done in Google Earth Engine, while modeling and visualization are carried out using Python. The output maps are intended for integration into terrain-aware navigation and planning systems.**

Keywords—Permafrost Mapping, TTOP, MAGT, ALT, Remote Sensing, Google Earth Engine, ERA5, Digital Elevation Model, NDVI, NDSI, Terrain Analysis, Arctic, Western Himalayas, Russia.

I. INTRODUCTION

Permafrost refers to ground that remains continuously frozen for two or more consecutive years. It is a critical factor influencing geotechnical stability, hydrological regimes, and terrain accessibility in cold regions. While global studies on permafrost have primarily focused on Arctic and sub-Arctic regions, recent attention has shifted to high-altitude mountain systems such as the Himalayas, where permafrost conditions exist above 3500 m elevation. Unlike polar regions, high-altitude permafrost is governed by complex terrain, variable snow cover, and microclimatic influences, making its detection and monitoring more challenging.

In regions such as the Western Himalayas and the Eastern Karakoram, permafrost zones overlap with forward operational areas of the Indian Armed Forces. Terrain instability due to thawing permafrost has been associated with slope failure, infrastructure degradation, and seasonal accessibility loss. However, due to the limited presence of in-situ borehole measurements and permanent monitoring stations in these zones, the spatial distribution and temporal behavior of permafrost remain poorly understood. This lack of data directly impacts strategic planning for road construction, fuel depots, communication infrastructure, and autonomous system mobility.

The objective of this work is to develop a geospatial framework for high-resolution permafrost probability mapping using publicly available satellite datasets, climate reanalysis products, and empirical thermal models. The approach integrates terrain elevation, slope, vegetation and snow indices, and temperature-based thermal indicators to generate permafrost classification layers for operational terrain. The methodology is applied to two study area namely the Indian Western Himalayas and the Russian Yamal region to evaluate performance in both high-altitude and Arctic environments.

Prior studies such as Brown et al. [1] established zonal classification schemes for global permafrost, while Smith and Riseborough [2] introduced the TTOP model for estimating subsurface temperature using mean annual air temperature (MAAT) and surface insulation parameters. Khan et al. [3] modeled permafrost distribution in the Western Himalaya using a combination of MODIS LST, slope, aspect, and land cover. Westermann et al. [4] combined MODIS-derived surface temperature with NDVI to infer ground thermal states. Luo et al. [5] developed the PIC R-package to compute thermal indices including FDD and ALT. However, most of these studies either focus on large-scale global datasets or lack detailed validation in Himalayan terrain.

Indian contributions to permafrost modeling remain limited. The Wadia Institute and other regional institutions have used short-term satellite data and empirical correlations to identify frost-prone zones in Ladakh. These efforts, however, are hindered by coarse spatial resolution, lack of calibration data, and insufficient modeling integration. Furthermore, national-level geoportals such as ISRO's Bhuvan provide terrain and snow datasets, but do not support direct permafrost mapping.

This study aims to fill this gap by implementing a modular, satellite-based permafrost modeling framework using TTOP, MAGT, and ALT as core thermal indicators. The framework is built on Google Earth Engine for data acquisition and Python-based spatial modeling for downstream processing. The output includes probability-classified permafrost maps, intended for integration into high-altitude logistics, route planning, and risk assessment workflows. By addressing both regional mapping challenges and operational requirements, this work supports defense-focused terrain analysis under changing climatic conditions.

II. Study Region and Data Sources

A. Regions of Interest

Two distinct regions were selected for permafrost probability modeling to test the framework across different climatic and topographic settings. The first region covers the high-altitude sectors of the Western Himalayas, encompassing Ladakh and northern Himachal Pradesh. The area of interest is bounded by 75.5°E to 80.5°E longitude and 28.5°N to 36.5°N latitude. This region features rugged topography, elevations above 3500 m, and limited vegetation cover.

The second region lies in the Arctic permafrost belt of Russia, specifically the Yamal Peninsula and surrounding zones between 75.5°E to 80.5°E longitude and 67.0°N to 71.0°N latitude. This region represents a predominantly continuous permafrost zone with tundra vegetation, flat terrain, and shallow active layers.

These contrasting regions allow for testing the same modeling approach in both high-altitude and high-latitude settings.

B. Terrain and Remote Sensing Inputs

Table I summarizes the key datasets used in this study. All inputs were processed and resampled to a common spatial resolution of 30 meters.

TABLE I. Input Description

Data type	***Dataset Name***	***Permafrost Indicator***	***Native Resolution***
Elevation	SRTM DEM, ASTER GDEM	Elevation, slope, aspect	30 m
Land Surface Temperature	MODIS MOD11A	8-day composite LST (Kelvin)	1 km
Vegetation Index	MODIS MOD13Q1	NDVI composite	250 m
Snow Cover	Landsat-8 SR, Sentinel-2	NDSI from visible/SWIR bands	30 m
Climate Reanalysis	ERA5-Land Daily 2m Temperature	Daily mean temp for FDD/TDD calculation	~ 9 km
Soil Properties	SoilGrids v2.0	Bulk density, clay, coarse fragments	250 m – 1 km

C. Data Preprocesssing and Alignment

All raster datasets were clipped to the regional boundaries and resampled to a 30 m spatial resolution using bilinear or cubic interpolation. MODIS and ERA5 products were downscaled and corrected using lapse rate methods to improve alignment with local terrain. Vegetation (NDVI) and snow cover (NDSI) indices were computed using spectral band ratios and composited seasonally. Terrain derivatives such as slope and aspect were generated using standard DEM processing tools. All inputs were standardized and converted to consistent projection formats to allow pixel-wise computations.

III. Methodology

The methodology follows a modular geospatial modeling pipeline designed to compute permafrost probability using satellite and reanalysis data. It includes preprocessing of raster inputs, computation of empirical indices, and integration into a probability map.

A. Workflow Overview

The first stage, Input Acquisition, collects all necessary geospatial and environmental datasets. Satellite-based land surface temperature data are sourced from MODIS, while vegetation and snow indices such as NDVI and NDSI are extracted from MODIS, Landsat-8, or Sentinel-2 imagery. ERA5-Land reanalysis data is used to obtain daily 2 m air temperatures for thermal modeling. Terrain information is gathered from Digital Elevation Models (DEM) such as SRTM or ASTER, and soil characteristics including bulk density, clay content, and coarse fragments are retrieved from the SoilGrids v2.0 database as observed in figure 1. The stages are as follows:

- In the **Preprocessing and Alignment** stage, all raster datasets are spatially clipped to match the defined Region of Interest (ROI) and resampled to a uniform 30-meter resolution using bilinear or cubic interpolation. Invalid pixels, such as those obscured by clouds or water bodies, are masked out. To ensure compatibility in modeling, variables like slope and elevation are normalized to a common scale, typically between 0 and 1.
- The **Index Derivation** stage transforms raw datasets into geophysically relevant indices. Land surface temperature is averaged over a multi-year window to estimate Mean Annual Air Temperature (MAAT). Terrain derivatives, including slope and aspect, are computed from the DEM. NDVI and NDSI are derived from optical imagery to assess vegetation cover and snow persistence, respectively. ERA5 temperature data, corrected using a lapse rate of –6.5 °C/km to account for elevation, is used to compute Freezing Degree Days (FDD) and Thawing Degree Days (TDD), which represent cumulative cold and warm temperature effects over a year.
- The **Empirical Modeling** stage applies three separate models to estimate key permafrost indicators. The Temperature at the Top of Permafrost (TTOP) is calculated using MAAT, surface insulation factors (n-factors), and thermal conductivity values derived from soil parameters. Mean Annual Ground Temperature (MAGT) is estimated through a regression-based model that incorporates NDVI, slope, LST, and elevation. Active Layer Thickness (ALT) is computed using Stefan's equation, incorporating FDD, bulk density, and soil conductivity to estimate annual thaw depth.
- In the **Integration and Probability Mapping stage**, the outputs from the three models (TTOP, MAGT, and ALT) are normalized. ALT is inverted since shallower thaw depths imply higher permafrost stability. These values are then combined into a unified permafrost probability score. The formula used is the mean of the three components: normalized TTOP, normalized MAGT, and (1 –

ALT/5). The resulting continuous probability map is classified into high, moderate, or low-confidence permafrost zones using empirical thresholds.

- Finally, the **Output and Visualization** stage prepares the model outputs for interpretation and use in defense applications. GeoTIFFs of TTOP, MAGT, ALT, and the composite probability map are generated. Classification masks are produced in both binary and trinary formats. Annotated overlays include geographic place names, slope and elevation bands, and other strategic references. These outputs are designed for further integration into autonomous path planning systems and terrain analysis platforms.

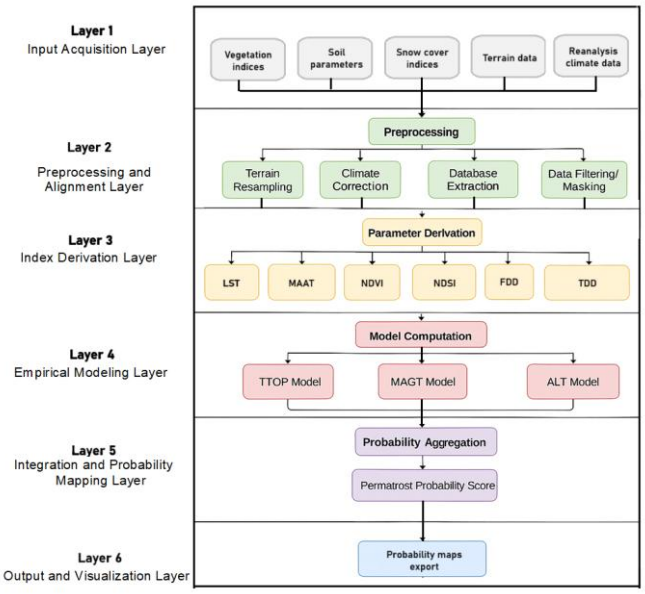

Fig. 1. Workflow chart

B. *Terrain and Vegetation Index Computation*

Accurate representation of terrain and land cover conditions is essential for modeling permafrost presence, as these variables influence ground energy balance, snow retention, and soil insulation. The following indices are derived from remote sensing datasets:

1) Slope (θ) : Slope represents the steepness of the terrain and affects water runoff, snow accumulation, and surface insulation.

$$\theta = \tan^{-1}\left(\sqrt{\left(\frac{\partial z}{\partial x}\right)^2 + \left(\frac{\partial z}{\partial y}\right)^2}\right) \quad (1)$$

Where:

dZ/dx : Elevation gradient in the x-direction
dZ/dy : Elevation gradient in the y-direction
θ : slope in radians (converted to degrees for interpretation)

Higher slope values typically correlate with faster snow shedding and reduced insulation, leading to lower permafrost stability.

2) Aspect (ϕ) : Aspect defines the direction a slope faces and influences solar radiation exposure.

$$\phi = \tan^{-1}\left(\frac{-\frac{\partial z}{\partial y}}{\frac{\partial z}{\partial x}}\right) \quad (2)$$

Where:

dZ/dx : Elevation gradient in the x-direction
dZ/dy : Elevation gradient in the y-direction
ϕ: terrain aspect angle (azimuth)
North-facing slopes ($\phi \approx 0°$ or 360°) receive less sunlight, favoring permafrost conditions in the Northern Hemisphere.

3) Normalized Difference Vegetation Index (NDVI): NDVI measures vegetation density and type, which influence the thermal resistance of the ground surface.

$$\text{NDVI} = \frac{NIR - RED}{NIR + RED} \quad (3)$$

Where:

NIR: reflectance in near-infrared band

RED: reflectance in red band

NDVI values range from −1 to +1, where higher values indicate denser vegetation. Vegetation acts as an insulating layer and impacts the freezing/thawing n-factors used in TTOP modeling

4) Normalized Difference Snow Index (NDSI): It identifies snow-covered areas, critical for estimating surface insulation in winter.

$$\text{NDSI} = \frac{GREEN - SWIR}{GREEN + SWIR} \quad (4)$$

Where:

GREEN: reflectance in green band

SWIR: reflectance in short-wave infrared band

High NDSI values (typically >0.4) indicate persistent snow. Snow modifies heat transfer into the ground and influences TTOP and MAGT estimates.

C. *Thermal Variable Estimation*

Thermal indices reflect the heat dynamics affecting soil freezing and thawing. These variables are essential for calculating empirical permafrost models like TTOP, MAGT, and ALT.

1) Mean Annual Air Temperature (MAAT): MAAT provides a base estimate of regional coldness, derived from long-term surface temperature data.

$$\text{MAAT} = \frac{1}{N}\sum_{i=1}^{N} LST_i - 273.15 \quad (5)$$

Where:

LST_i : MODIS Land Surface Temperature for day i (in Kelvin)
N: total number of valid observations
Converted to °C by subtracting 273.15

MAAT is used directly in the TTOP model to estimate subsurface freezing conditions.

2) Lapse-Rate Corrected ERA5 Temperature: To correct coarse ERA5 air temperature data for local elevation differences, a standard lapse rate is applied:

$$T_{\text{corrected}} = T_{\text{ERA5}} - \Gamma \cdot (h_{\text{DEM}} - h_{\text{ERA5}}) \quad (6)$$

Where:

T_{ERA5} : reanalysis temperature at coarse resolution
$\Gamma = 6.5^{\circ}\, C/km$: standard atmospheric lapse rate
h_{DEM} : elevation at pixel from DEM
h_{ERA5} : average ERA5 elevation for the grid cell

Corrected temperatures improve spatial accuracy when computing FDD and TDD.

3) Freezing Degree Days (FDD): FDD quantifies the cumulative cold required for ground freezing.

$$\text{FDD} = \sum_{i=1}^{n} \max(0, -T_i) \quad (7)$$

Where:

Ti : daily mean air temperature (in °C)

Only temperatures below 0°C are considered. FDD is used in ALT modeling and represents energy loss to the ground surface.

4) Thawing Degree Days (TDD): TDD represents cumulative warming during thawing seasons.

$$\text{TDD} = \sum_{i=1}^{n} \max(0, T_i) \quad (8)$$

Where:

Ti : daily mean air temperature (in °C)

Only temperatures above 0°C are accumulated. Higher TDD implies greater active layer thickness (ALT) and reduced permafrost probability.

D. Empirical Models

1) TTOP Equation and Normalization: It is computed using the following model:

$$TTOP = \text{MAAT} \cdot n_f - n_t \cdot \left(\frac{K_t}{K_f}\right) \quad (9)$$

Where:

MAAT is derived from MODIS LST (in °C)
nf, nt are n-factors estimated from NDVI and NDSI
Kf, Kt are thermal conductivities

This semi-empirical model estimates the temperature at the freezing boundary below the active layer. A negative TTOP (< 0°C) implies stable permafrost conditions. The resulting raster is normalized using:

$$TTOP_{norm} = \frac{TTOP - TTOP_{min}}{TTOP_{max} - TTOP_{min}} \quad (10)$$

This allows the value to contribute equally when integrated with other maps.

2) ALT Estimation via Stefan's Law: ALT represents the depth to which seasonal thawing occurs and is calculated using:

$$ALT = \sqrt{\frac{2 \cdot k \cdot FDD}{\rho \cdot L_f}} \quad (11)$$

Where:

k = average thermal conductivity = $0.5 \cdot (Kf + Kt)$
FDD = Freezing Degree Days
ρ = bulk density
Lf = latent heat of fusion for water (334,000 J/kg)

Higher FDD implies a deeper freeze, but higher soil density and conductivity can buffer thaw. A threshold of ALT < 1.5 m is used to classify high-confidence permafrost zones. ALT is clipped between 0 and 5 meters and also used as an inverse component in the final composite score:

$$ALT_{inv} = 1 - \left(\frac{ALT}{5}\right) \quad (12)$$

3) MAGT Weighted Empirical Regression: MAGT (Mean Annual Ground Temperature) is approximated using a weighted regression model:

$$MAGT = \alpha \cdot LST + \beta \cdot NDVI + \delta \cdot \text{slope}_{norm} + \epsilon \cdot \text{elevation}_{norm} + C \quad (13)$$

Where empirically tuned coefficients are $\alpha = -1.5$, $\beta = -2.2$, $\delta = -0.5$, $\epsilon = -0.2$, $C = 5.0$. These values were adapted from literature and validated against known regional thermal behavior. The regression reflects that high NDVI, low elevation, and low slope lead to warmer ground temperatures. The output MAGT is then normalized to [0,1] like the TTOP layer:

E. Probability Score Computation

The composite permafrost probability (P) is calculated as:

$$P = \frac{1}{3}\left[\text{norm}(TTOP) + \text{norm}(MAGT) + \left(1 - \frac{ALT}{5}\right)\right] \quad (14)$$

This simple average assumes equal weight for each indicator, which is justified given their complementary roles:

- TTOP reflects thermal boundary behavior.
- MAGT captures average sub-surface thermal regime.
- ALT reflects the physical outcome of freeze-thaw energy balance.

The probability scores are clipped between 0 and 1. They are then classified into:

- High Confidence (P > 0.7)
- Moderate Confidence (0.7 < P ⩽ 0.4)
- Low Confidence (P ⩽ 0.4)

Each class is mapped as a different raster layer. These masks are then exported and visualized using color-coded overlays for intuitive interpretation.

IV. Implementation and Visualization

A. Data Preprocessing in Google Earth Engine

Google Earth Engine (GEE) was used for initial data acquisition and preprocessing due to its support for multi-sensor satellite datasets and large-scale geospatial computations. The Region of Interest (ROI) was defined separately for India (75.5°E–80.5°E, 28.5°N–36.5°N) and Russia (75.5°E–80.5°E, 67.0°N–71.0°N). The following datasets were processed:

- DEM: SRTM 30 m elevation data for slope and aspect calculations.
- Thermal Data: MODIS MOD11A2 8-day LST composites (1 km), averaged over 2020–2023.
- Vegetation Index: MOD13Q1 NDVI, seasonally maximized to reflect peak vegetation.
- Snow Cover Index: Landsat-8 NDSI, derived from median winter composites with cloud filtering.
- Climate Reanalysis: ERA5-Land daily 2 m temperature, used to compute Freezing Degree Days (FDD) and Thawing Degree Days (TDD) after applying lapse-rate corrections.

All datasets were resampled to 30 m resolution and exported as GeoTIFFs to Google Drive for further processing.

B. Raster Stack Creation and Standardization

In the local Python environment, raster stacks were created by aligning all exported datasets to a common grid using rasterio and numpy. The DEM was used as the reference raster. All other rasters were resampled using bilinear interpolation. Nodata values were replaced with zeros or threshold-based values to avoid model instability. Each raster layer was normalized to prepare for modeling.

C. Empirical Model Implementation

Three models were independently implemented in Python as discussed in the methodology and their composite permafrost probability index generates the required map.

D. Map Rendering and Overlays

Final outputs were visualized using Python libraries such as matplotlib, geopandas, and shapely using the following:

Color Palettes:

- TTOP, MAGT: coolwarm (range: −20°C to +20°C)
- ALT: magma (range: 0–5 m)
- Probability Map: plasma or viridis
- Classified Zones: gray (low), orange (moderate), dark red (high)

Overlays:

- Place names such as Leh, Kargil, Salekhard, and Nadym were geocoded and added as raster annotations.
- Elevation contours and slope masks were superimposed for geotechnical context.
- Each figure was saved as a high-resolution PNG and GeoTIFF and integrated into the path planning module for autonomous navigation applications.

V. Results

Preliminary data that was acquired and preprocessed (LST, NDVI, NDSI, Slope, Aspect, Soil Bulk density, Clay fraction and Coarse fragment) are as seen in figures 2 to 8 for the sample area of 75.5°E to 80.5°E, 36.5°N to 32.5°N in India along with the three key indicators namely TTOP (Temperature at the Top of Permafrost), MAGT (Mean Annual Ground Temperature), and ALT (Active Layer Thickness) and their combined composite permafrost probability map along with binary classification map as seen in figures 9 to 13 for and figure 14 shows composite probability map for India 75.5°E to 80.5°E, 32.5°N to 28.5°N while 6.15 shows composite probability map for Russia 75.5°E to 80.5°E, 67.0°N to 71.0°N:

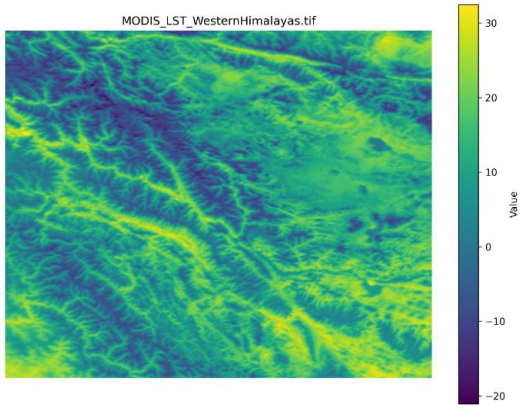

Fig. 2. Land Surface Temperature

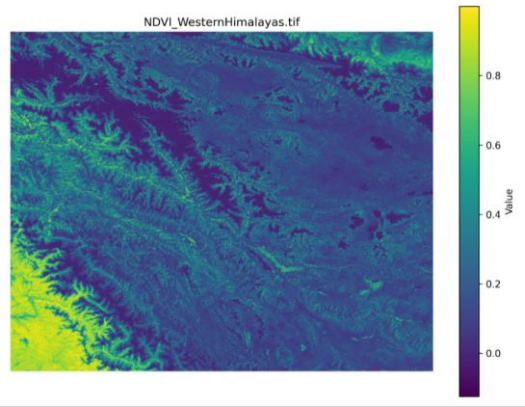

Fig. 3. Normalized Difference Vegetation Index

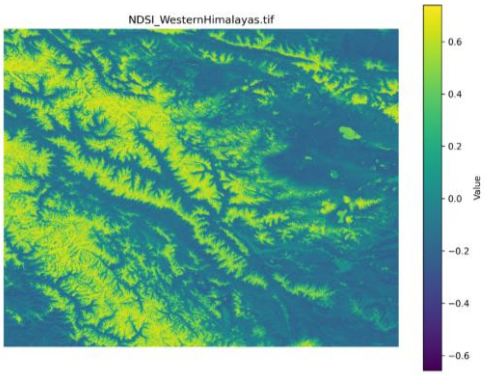

Fig. 4. Normalized Difference Snow Index

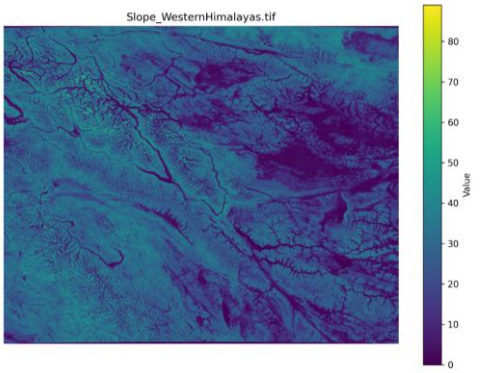

Fig. 5. Slope

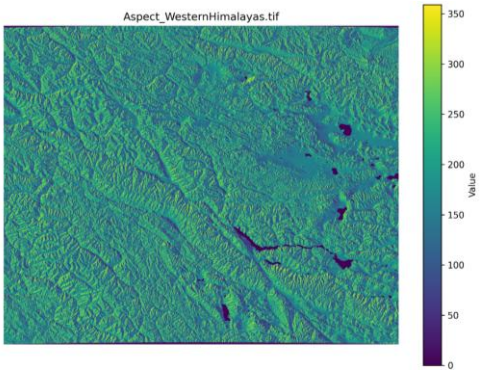

Fig. 6. Aspect

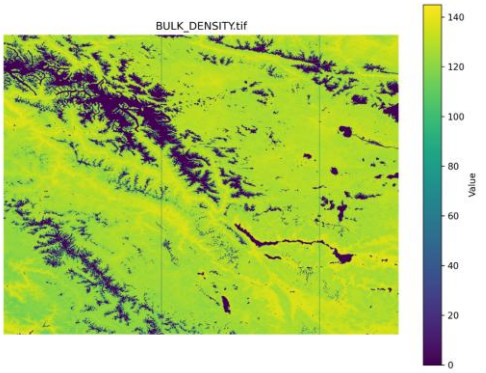

Fig. 7. Soil Bulk density

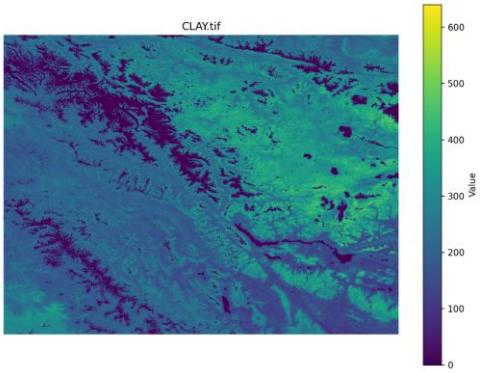

Fig. 8. Clay fraction

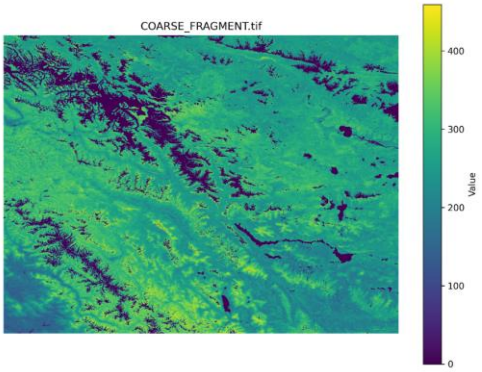

Fig. 9. Coarse fragment

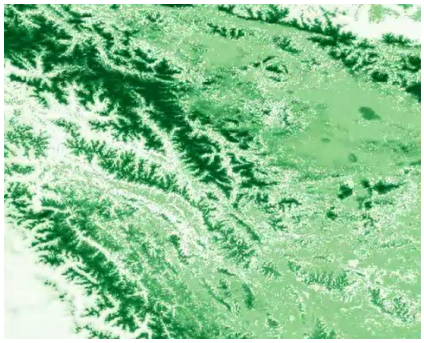

Fig. 10. ALT map

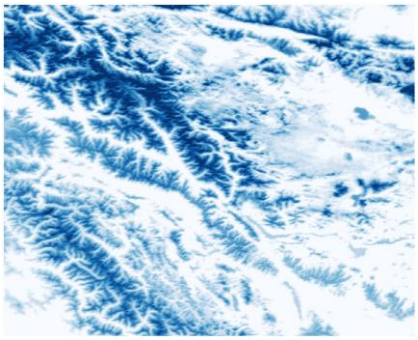

Fig. 11. MAGT map

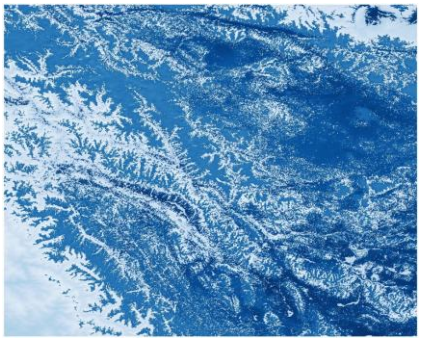

Fig. 12. TTOP map

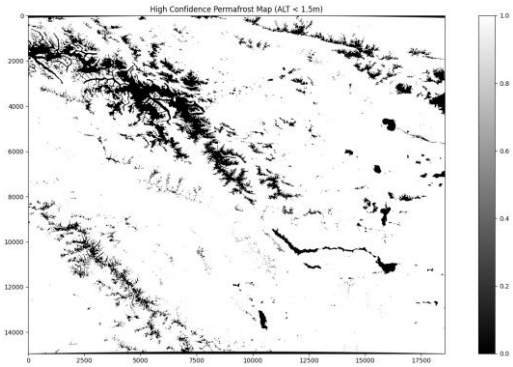

Fig. 13. Binary permafrost zone classification

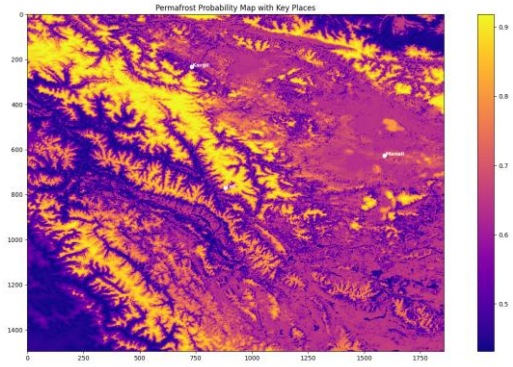

Fig. 14. Composite permafrost probability map India 1

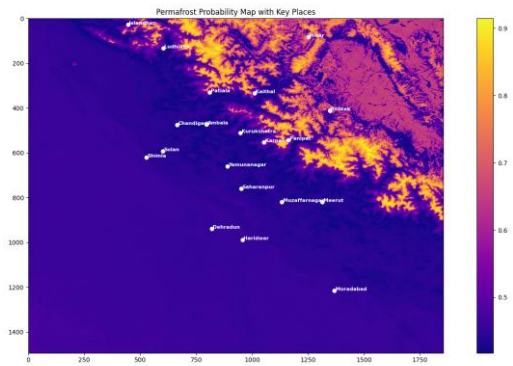

Fig. 15. Composite permafrost probability map India 2

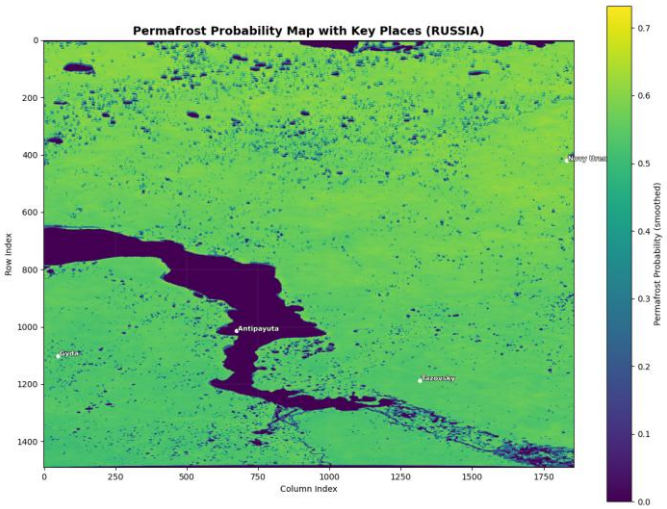

Fig. 16. Composite permafrost probability map Russia

The zonation for each model was based on established literature thresholds and field-calibrated proxies. Classification was carried out using NumPy masking and raster reclassification within the Python modeling environment.

TTOP Zones:

- TTOP ≤ −2 °C: Very High likelihood of permafrost presence
- −2 °C < TTOP ≤ 0 °C: Moderate likelihood
- TTOP > 0 °C: Low likelihood or no permafrost

MAGT Zones:

- MAGT ≤ −1.5 °C: Stable or continuous permafrost zone
- −1.5 °C < MAGT ≤ 0.5 °C: Marginal/discontinuous zone
- MAGT > 0.5 °C: Likely unfrozen ground

ALT Zones:

- ALT < 0.5 m: Stable permafrost (perennially frozen)
- 0.5 m ≤ ALT < 1.5 m: Seasonal/marginal stability
- ALT ≥ 1.5 m: Deep thaw layer; no reliable permafrost

To ensure the reliability of the modeled permafrost indicators—ALT (Active Layer Thickness), MAGT (Mean Annual Ground Temperature), and the derived permafrost probability maps—we conducted a comparative analysis with authoritative global datasets such as those from ESA and NIEER. The focus was to validate spatial correspondence and pattern accuracy across both Indian and Russian regions.

Fig. 17. ESA MAGT Map for Yamal Region, Russia

Fig. 17 illustrates the MAGT distribution obtained from the ESA Permafrost CCI dataset for the Russian Yamal region. This dataset represents climatologically averaged MAGT values interpolated using borehole observations and satellite-derived predictors.

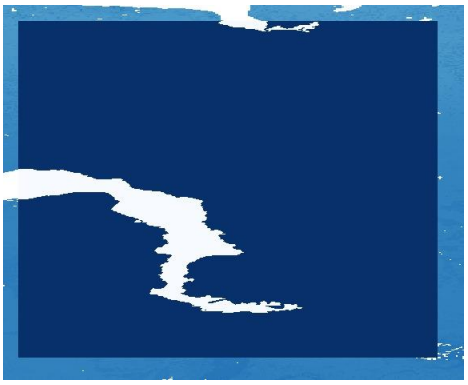

Fig. 18. Locally Computed MAGT Map using MODIS and Terrain Derivatives

Fig. 18 shows the MAGT map generated from our model using calibrated regression on MODIS LST, NDVI, normalized slope, and DEM elevation.

Inference: The spatial temperature gradients show good correlation, particularly in zones with persistent permafrost. Northern regions show low MAGT values (below -5 °C), while southern areas reflect warmer ground conditions. Our model provides finer spatial resolution and better terrain discrimination due to the incorporation of slope and NDVI.

Fig. 19. ALT Map from NIEER Database – Russian Permafrost Domain

Fig. 20. Computed ALT Map

Fig. 20 presents our computed ALT map using the Stefan equation, with FDD, bulk density-based thermal conductivity, and soil parameters.

Inference: The pattern of shallow active layers (ALT < 1.5 m) in permafrost-prone zones aligns well in both maps. Notable agreement is observed in the northern tundra zones and riverbank regions. Variations near the southern margin arise due to interpolation differences in NIEER versus our grid-based approach using satellite datasets.

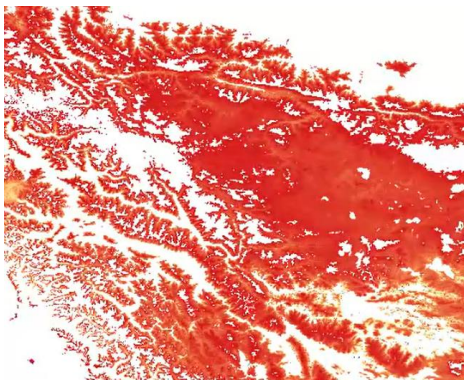

Fig. 21. ESA ALT Map for the Indian Western Himalayas

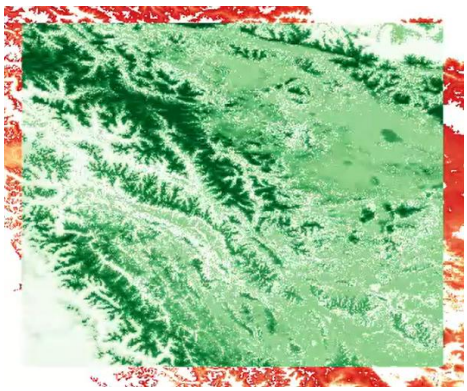

Fig. 22. Computed ALT Map

Inference: Our model replicates the ESA trends in ALT depth, especially around Leh, Kargil, and Lahaul-Spiti. Low-ALT zones in our map coincide with high-altitude plateaus and north-facing slopes, reflecting areas of strong permafrost likelihood. Our use of high-resolution inputs enables better detection of local thermal variations within narrow valleys and ridge lines.

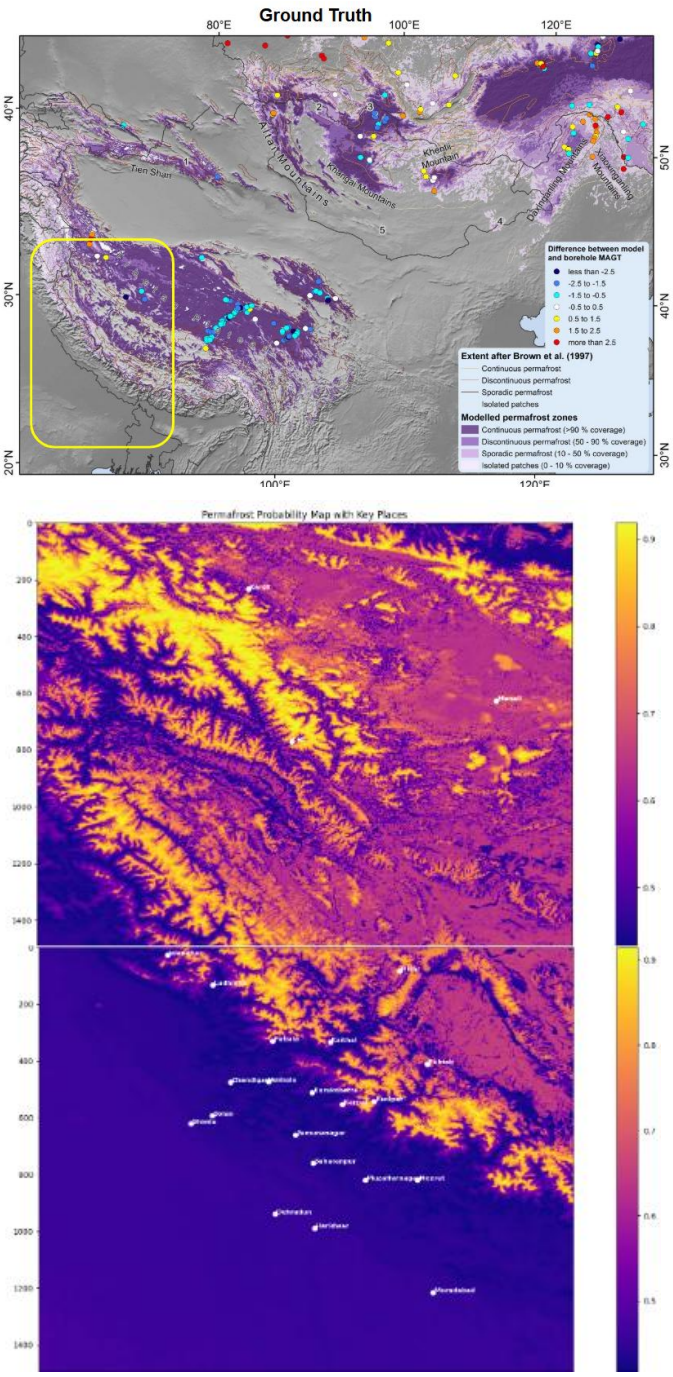

Fig. 23. Compared Permafrost Probability Map – Western Himalayas

Fig. 23 presents the combined permafrost probability map for the Indian region, based on a weighted integration of MAGT, TTOP, and ALT indicators.

Inference: Regions with high permafrost probability (scores > 0.7) strongly correspond to known cryosphere zones, including Ladakh and upper Lahaul. Compared to standalone ALT or MAGT maps, the ensemble model reduces ambiguity in marginal areas by capturing complementary aspects of thermal state and seasonal thaw dynamics.

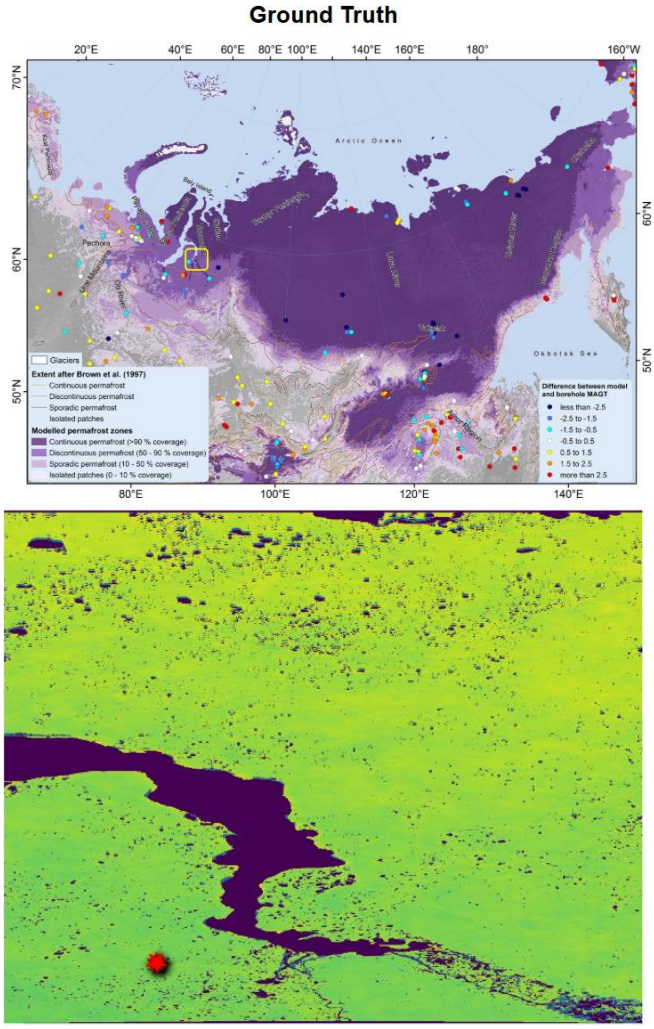

Fig. 24. Compared Permafrost Probability Map – Russia

Fig. 24 shows the permafrost probability map for the Yamal Peninsula in Russia using our integrated approach.

Inference: Northern Arctic zones (e.g., Sabetta, Tazovsky) show high permafrost stability (scores > 0.85), while transitional bands toward Novy Urengoy and Nadym reflect reduced stability with probability between 0.4 and 0.6. These results match expected gradients and enhance prediction clarity compared to conventional single-variable thresholds.

VI. Conclusion and Future Work

A. *Conclusion*

This study presents a structured methodology for high-resolution permafrost probability mapping in two climatically distinct high-latitude and high-altitude regions—India's Western Himalayas and Russia's Yamal Peninsula. Using a combination of satellite imagery (MODIS, Landsat), reanalysis climate data (ERA5), digital elevation models (SRTM/ASTER), and soil datasets (SoilGrids), the research implements a layered geospatial pipeline that transforms raw environmental variables into thermal indicators and ultimately into permafrost probability classifications.

Three empirical models—TTOP, MAGT, and ALT—were derived using a combination of terrain, vegetation, and temperature-based indices. These were then normalized and

fused into a composite probability score to map the likelihood of permafrost presence. The results were visualized using classified outputs (high, moderate, low probability zones) and interpreted in conjunction with terrain and climatological context. The maps generated provide valuable terrain intelligence that may support defense logistics, autonomous vehicle routing, and environmental monitoring.

The findings show clear spatial variation in permafrost occurrence linked to elevation, slope orientation, vegetation cover, and temperature profiles. While the Western Himalayas exhibit fragmented permafrost in high-altitude pockets above 4,000 m, the Russian Arctic presents broader zones of near-continuous permafrost. These outputs demonstrate the potential of integrated empirical modeling combined with remote sensing data for scalable terrain classification.

B. *Future Work*

Several avenues for future enhancement were identified:

- Model Calibration with Field Data: The current models were validated visually and statistically using global references but not calibrated with borehole or ground-truth datasets in the Indian region. Future deployments should incorporate field sensors or field expeditions to validate MAAT, MAGT, and ALT predictions.
- Machine Learning Integration: Future work can incorporate supervised learning models trained on borehole or manually classified maps to improve classification boundaries and compensate for limitations in empirical parameterizations.
- Seasonal Monitoring and Change Detection: Extending the temporal range and implementing seasonal monitoring would allow tracking of permafrost degradation, active layer variability, and snow persistence dynamics under changing climate scenarios.
- Expansion to Other Regions: The modular architecture allows replication of the methodology in other cold regions like Central Asia, Antarctica, and the Andes by replacing regional datasets. Automated scaling with cloud processing (e.g., Google Earth Engine) enables quick redeployment.
- Defense Path Planning Systems Integration: The generated probability maps can be directly fed into path planning frameworks such as terrain-aware A*, Hybrid A*, or behavior-based planners used in autonomous defense vehicles. This will enhance mobility decisions in geotechnically unstable terrains.
- Use of Synthetic Aperture Radar (SAR): Sentinel-1-based SAR backscatter or InSAR data can improve detection of seasonal freeze-thaw subsidence and surface instability, supplementing the thermal models used here.
- Higher-Resolution Inputs: Newer datasets such as ECOSTRESS thermal products, TanDEM-X DEM, or downscaled ERA5 datasets can offer finer spatial resolution and improve the accuracy of terrain and temperature modeling.

In summary, this work provides a reproducible and extensible framework for permafrost probability estimation using publicly available datasets and can be used to support climate adaptation, terrain risk assessment, and autonomous mobility in fragile regions.

REFERENCES

[1] M. A. R. Khan, B. S. Sinha, and A. K. Patel, "Modelling Permafrost Distribution in Western Himalaya Using Remote Sensing and Field Observations," Remote Sensing, vol. 13, no. 14, pp. 1–22, 2021.

[2] D. Luo, Z. Wu, X. Li, and H. Liu, "PIC v1.3: Comprehensive R Package for Computing Permafrost Indices over the Qinghai–Tibet Plateau," Geoscientific Model Development, vol. 14, no. 3, pp. 1379–1396, 2021.

[3] J. Brown, O. J. Ferrians Jr., J. A. Heginbottom, and E. S. Melnikov, "Circum-Arctic Map of Permafrost and Ground-Ice Conditions," National Snow and Ice Data Center, Boulder, CO, 1997

[4] M. W. Smith and D. W. Riseborough, "Climate and the Limits of Permafrost: A Zonal Analysis," Permafrost and Periglacial Processes, vol. 13, no. 1, pp. 1–15, 2002.

[5] T. Zhang, R. G. Barry, K. Stamnes, V. Romanovsky, and M. T. Prowse, "Spatial and Temporal Variability in Active Layer Thickness," Journal of Geophysical Research: Atmospheres, vol. 110, no. D13, pp. 1–13, 2005.

[6] N. Gorelick et al., "Google Earth Engine: Planetary-Scale Geospatial Analysis for Everyone," Remote Sensing of Environment, vol. 202, pp. 18–27, 2017.

[7] S. Westermann, R. Kumar, and T. J. Frolking, "Remote Sensing of Permafrost and Frozen Ground," Earth Science Reviews, vol. 147, pp. 330–354, 2015.

[8] T. E. Osterkamp, "Characteristics of the Recent Warming of Permafrost in Alaska," Journal of Geophysical Research: Earth Surface, vol. 112, F02S02, 2007.

[9] ISRO - National Remote Sensing Centre, "Bhuvan Geoportal," [Online]. Available: https://bhuvan.nrsc.gov.in

[10] Wadia Institute of Himalayan Geology (WIHG), "Studies on Permafrost in the Western Himalayas," Technical Report, 2020.

[11] A. Negi, S. K. Srivastava, and R. D. Singh, "Snow and Permafrost Studies in Ladakh Using Remote Sensing," International Journal of Remote Sensing Applications, vol. 11, no. 2, pp. 45–57, 2021.

[12] H. Hersbach et al., "The ERA5 Global Reanalysis Dataset," Quarterly Journal of the Royal Meteorological Society, vol. 146, no. 730, pp. 1999–2049, 2020.

[13] A. Lewkowicz and J. Bonnaventure, "Permafrost and Climate Change in Canada: An Overview of Recent Research and Future Trends," Canadian Journal of Earth Sciences, vol. 45, no. 10, pp. 1213–1230, 2008.

[14] G. Hugelius et al., "The Northern Circumpolar Soil Carbon Database: Spatially Distributed Datasets of Soil Coverage and Soil Organic Carbon Storage in the Northern Permafrost Regions," Earth System Science Data, vol. 5, no. 1, pp. 3–13, 2013.

[15] M. Jafarov, V. E. Romanovsky, and J. E. Walsh, "Permafrost Degradation and Modeled Soil Carbon Loss in the West Siberian Arctic Region," Geophysical Research Letters, vol. 39, no. L05503, pp. 1–6, 2012.

[16] T. Zhang and R. G. Barry, "The Sensitivity of Permafrost to Climate Change: Empirical Relations from Observations and Simulations," Climatic Change, vol. 52, no. 1–2, pp. 161–182, 2002.